

Wind Shear, Gust, and Yaw-Induced Dynamic Stall on Wind-Turbine Blades

B. P. laBastide, J. G. Wong and D. E. Rival

Department of Mechanical and Materials Engineering, Queen's University, Kingston, ON,
Canada K7L 3N6

E-mail: jaime.wong@queensu.ca

Abstract. This study examined the effect of a spanwise angle of attack gradient on the growth and stability of a dynamic stall vortex on a rotating blade. It was found that a spanwise angle of attack gradient induces a corresponding spanwise vorticity gradient, which, in combination with spanwise flow, results in a redistribution of circulation along the blade. Specifically, when replicating the angle of attack gradient experienced by a wind turbine at the 30% span position during a gust event, the spanwise vorticity gradient was aligned such that circulation was transported from areas of high circulation to areas of low circulation. This in turn increased the local dynamic stall vortex growth rate, which corresponds to an increase in the lift coefficient, and a decrease in the local vortex stability at this point. Reversing the relative alignment of the spanwise vorticity gradient and spanwise flow results in circulation transport from towards areas of high circulation generation, which acted to reduce local circulation and thereby stabilize the vortex. This circulation redistribution behaviour describes a mechanism by which the fluctuating loads on a wind turbine are magnified, which is detrimental to turbine lifetime and performance.

1. Introduction

Modelling wind turbine performance and subsequently determining design specifications for turbine blades is most often performed using blade element models [1]. An inherent limitation in these models is that they assume little to no interaction between the blade elements, such that each element is treated as an independent two-dimensional airfoil section [2]. In reality, a turbine blade is a three-dimensional system with fluid and momentum transported along its span. This momentum transport is often modelled by correction factors, which use an empirical correction to account for this three-dimensional behaviour in steady operation [3, 4]. However, due to the empirical, as opposed to predictive, nature of these methods, such correction factors can not account for the highly unsteady detached flows one expects in gusty conditions, such as the formation of a dynamic stall vortex. This results in large errors from these models when predicting aerodynamic loading on turbine blades [5]. Additionally, such unsteady detached flows are responsible for the fatigue cycles with the highest peak-to-peak loading for both blade and rotor shaft bending, reducing turbine lifetime [6, 7]. Therefore, an understanding of the flow physics which dictate these forces would be beneficial in designing more reliable wind turbines. The remainder of this section will present a background on dynamic stall formation for rotating blades.



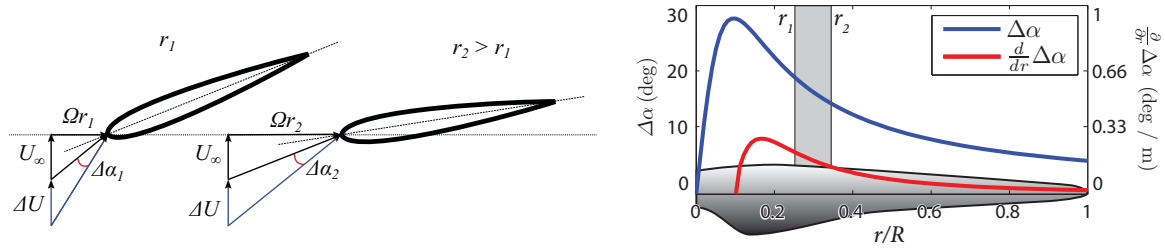


Figure 1. Relative angle-of-attack (α) change shown at two spanwise positions (left). A change in the axial velocity ΔU has a larger impact on angle-of-attack for smaller values of r/R . The resulting spanwise angle-of-attack magnitude and gradient change experienced by a turbine blade during a gust is shown in blue and red, respectively (right). The region investigated in this study is highlighted in grey with corresponding boundaries r_1 and r_2 indicated.

1.1. The Effect of Gusts on Angle of Attack

As a result of the transient conditions such as wind shear, gust, and turbine yaw, a turbine will experience rapid changes in angle of attack, which greatly influence the aerodynamic forces experienced by the blade. Under steady operating conditions, the turbine blade is designed to maintain a constant circulation profile over the span of the blade [8]. However, when a gust impinges on a blade the change in angle of attack across the blade $\Delta\alpha$ is highly non-uniform, following the relationship:

$$\Delta\alpha(r) = \arctan(U_\infty + \Delta U/\Omega r) - \alpha_0, \quad (1)$$

where $\Delta\alpha(r)$ is the change in angle of attack as a function of radius r , ΔU is the change in the free stream velocity, and α_0 is the initial angle of attack. This relationship is shown in Figure 1 for two spanwise positions r_1 and r_2 under a change in axial velocity ΔU . At an inboard (towards the hub) spanwise position r_1 the change in axial velocity ΔU has a larger impact on the effective velocity experienced by the blade section as the change in free-stream velocity ΔU is large in comparison to the velocity due to rotation Ωr_1 . Subsequently, inboard spanwise position r_1 experiences a greater change in angle of attack than a more outboard (towards the tip) spanwise position r_2 . In turn, spanwise position r_2 experiences a smaller change in the magnitude of the angle of attack.

When the angle of attack is calculated at all spanwise positions for a rotating blade experiencing a gust event, the spanwise gradient in angle of attack can be computed. As shown in Figure 1, both the change in magnitude and the spanwise gradient of angle of attack are largest in the near-root region, and decrease as a function of radius towards the tip of the blade resulting in the three-dimensional stall behavior discussed in the following section.

1.2. Three-Dimensional Dynamic Stall

In this study, we are primarily interested in the dynamic stall of wind turbines in gusty environments. Due to the spanwise angle of attack gradients outlined above, dynamic stall vortex evolution is a function of the spanwise position on the blade. Inboard locations, as described previously, experience higher effective angle of attack changes during a gust event, causing dynamic stall to initiate earlier [9]. Following stall initiation, higher effective angles of attack correspond to a higher rate of circulation generation, which corresponds to a higher rate of circulation growth within the dynamic stall vortex. As a result, and in the absence of spanwise interactions, the dynamic stall vortex at inboard locations would be expected to reach a length scale of one chord sooner than outboard positions, which has been identified as

a limiting length scale indicating the onset of vortex detachment [10]. This effect is reversed for other classes of rotating airfoils, such as in flapping wing flight where outboard positions experience a greater angle of attack change, corresponding to decreased stability at these points. However, as observed in both rotating and flapping systems, a persistent dynamic stall vortex is often generated on rotating and flapping profiles, which lasts for much larger time-scales in such three-dimensional cases than the two-dimensional case [11–15]. It has been proposed that rotational accelerations act to stabilize the vortex, with three critical rotational accelerations affecting vortex attachment [16]: the angular acceleration (a_{ang}), centripetal acceleration (a_{cen}), and Coriolis acceleration (a_{Cor}):

$$a_{ang} = \hat{\Omega} \times \hat{r}, \quad (2)$$

$$a_{cen} = \hat{\Omega} \times (\hat{\Omega} \times \hat{r}), \quad (3)$$

$$a_{Cor} = 2\hat{\Omega} \times u_{loc}, \quad (4)$$

where u_{loc} is the local velocity in the rotating frame. Note that in quasi-steady rotation cases the angular acceleration goes to zero $\hat{\Omega} = 0$. The centripetal acceleration a_{cen} induces a pressure gradient that drives spanwise flow. The local velocity u_{loc} is the sum of both the free stream velocity and that velocity induced by the flapping motion of the wing. In steady wind turbine operation, the free stream velocity is parallel the axis of rotation, and therefore does not contribute to the Coriolis acceleration, which becomes exclusively a function of the flow induced by the blade rotation:

$$a_{Cor} = 2\Omega \times u_{loc} = 2\Omega \times (\Omega \times r). \quad (5)$$

In a linear momentum balance described by the Navier-Stokes equation, the Coriolis effect acts to stabilize the dynamic stall vortex [17]. The current work uses an angular momentum balance, described by the vorticity transport equation, to examine a similar situation. Within this framework, the Coriolis effect is manifested as an induced spanwise flow [18]. Spanwise flow on the order of the flapping velocity can be expected, as this has been observed for dynamic stall vortices as in a flapping motion [11]. This spanwise flow contributes to the redistribution of vorticity along the span of the blade following the vorticity transport equation:

$$\frac{d\omega}{dt} + (\vec{u} \cdot \nabla)\omega = (\omega \cdot \nabla)\vec{u} + \nu \nabla^2 \vec{\omega}, \quad (6)$$

where the terms from left to right describe the change in vorticity of the fluid due to unsteadiness and convection, vortex tilting and stretching, and the viscous diffusion of vorticity, respectively. For a gust event acting on a rotating blade, viscous diffusion can be neglected under the assumption that the timescales of diffusion are much larger than the timescales of vortex growth itself. Therefore, the spanwise component of the vorticity transport equation in the rotating frame takes the form:

$$\frac{\partial \omega_r}{\partial t} + u_r \frac{\partial \omega_r}{\partial r} + \frac{u_\theta}{r} \frac{\partial \omega_r}{\partial \theta} + u_z \frac{\partial \omega_r}{\partial z} = \omega_r \frac{\partial u_r}{\partial r} + \frac{\omega_\theta}{r} \frac{\partial u_r}{\partial \theta} + \omega_z \frac{\partial u_r}{\partial z} + 2\Omega \frac{\partial u_r}{\partial z}, \quad (7)$$

where the terms from left to right are the constituent terms of Equation (6) above representing the rate of change of vorticity due to unsteadiness, the convection of vorticity in the r –, θ –, and z – directions, vortex tilting and vortex stretching, and Coriolis effects, respectively. A schematic of the hypothesised vorticity balance is shown in Figure 2, where circulation generated in the shear layer is balanced by spanwise vorticity convection. It can be assumed that the vortex is aligned approximately parallel with the span of the blade, and that therefore ω_r is the dominant component of vorticity present in the flow [19]. The rate of spanwise circulation redistribution

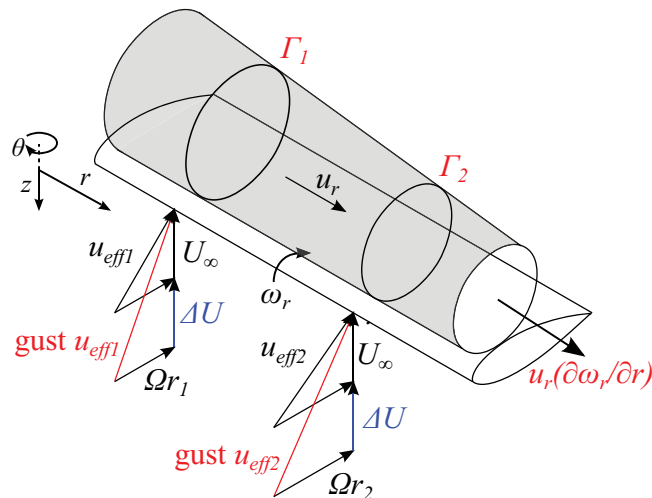


Figure 2. A section of a rotating turbine blade experiencing a gust event has a spanwise variation in angle of attack in the presence of radial flow, resulting in vorticity convection ($u_r \partial \omega_r / \partial r$) towards the blade tip.

can be computed by integrating the vorticity-transport equation across the vortex-core area [20, 19]:

$$\frac{\partial \Gamma}{\partial t} = - \int u_r \frac{\partial \omega_r}{\partial r} dA, \quad (8)$$

where the vortex tilting term vanishes as the vortex is aligned along the span of the blade and therefore vorticity is only minimally re-oriented. The stretching term vanishes, as stretching acts to increase centre line vorticity but does not transport vorticity along the blade span. Additionally, for a vortex tube attached near the leading edge of the blade profile, gradients in the spanwise direction will be much larger than the gradients in the streamwise direction, resulting in the Coriolis term having an negligible direct impact on spanwise vorticity transport. Note that Equation (8) considers only the change in circulation due to vorticity transport, in addition to circulation generated at any profile section.

As examined above, in transient flow conditions wind turbines develop a gradient in angle of attack along the blade span, from which a spanwise vorticity gradient is formed. It is postulated that, in combination with the spanwise flow induced by rotational accelerations, this spanwise vorticity gradient acts to redistribute circulation along the span of the blade towards the root. For inboard locations where the change in angle of attack $\Delta \alpha$ is greatest, this redistribution would result in a greater magnitude of local circulation at the, increasing the lift experienced at this location while reducing the stability of the dynamic stall vortex.

2. Methods

The angle of attack magnitude and spanwise gradient in angle of attack was determined for a reference 5MW NREL turbine operating at a free-stream velocity of $U_\infty = 11 \text{ m/s}$ experiencing a gust of $\Delta U = U_\infty$ at a reduced frequency of $k = \pi f c / U_\infty = 0.35$. This gust magnitude and frequency was chosen to be an extreme gust event, beyond what could be accommodated by pitch control. The change in angle of attack was determined for a sinusoidal variation in free-stream velocity of at the 30% span position. As a result, three test cases were developed. The first test case, hereafter referred to as the turbine case, was set up to exactly mimic the temporal

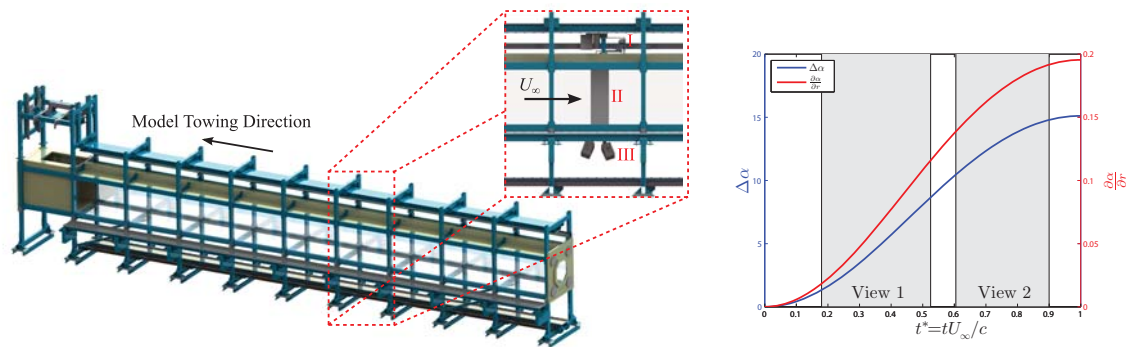


Figure 3. All test cases were conducted in a 15m long 1m \times 1m cross section towing tank. The model (II) was actuated using a robotic pitch flap mechanism (I), which was towed from right to left along the upper traverse. A 4 camera setup (III) was used to capture the motion of the seeding particles. An example angle of attack program is shown to the right.

angle of attack change, change in the spanwise gradient of angle of attack, and spanwise flow direction experienced at the 30% span of the reference 5MW turbine. This case was developed in order to visualize and quantify the effect of spanwise redistribution of circulation on a wind turbine blade.

The second test case, hereafter referred to as the flapping case, was set up such that the temporal angle of attack change, and thus the change in the spanwise gradient of angle of attack, was equal in magnitude but opposite in orientation to the reference turbine. The spanwise flow direction is identical in each case. The relative orientation of the spanwise vorticity gradient and the spanwise flow direction in this case is the same as that found in flapping systems such as birds and insects. This case was developed in order to contrast the turbine case, and is used to discuss the global behaviour of the spanwise circulation profile. The third test case, hereafter referred to as the reference case, was set up to be a quasi two-dimensional case with no spanwise gradient in angle of attack, while having a magnitude change in angle of attack equal to the other test cases. The angle of attack program for the turbine case is shown in Figure 3.

All tests were conducted in a 1m \times 1m cross section, optical towing tank shown in Figure 3. The tank is 15m long and uses water as the working fluid. The side and bottom walls of the tank are glass to allow for optical access. A traverse system, running the length of the towing tank, on which a 30cm chord NACA-0012 test article was mounted, is fixed above the tank and was ran at a Reynolds number of $Re_c = 10^5$, corresponding to a free-stream velocity of $U_\infty = 0.33\text{m/s}$. A pitch and flap actuator mechanism was mounted underneath this traverse system in order to control the blade motion, as shown in Figure 4. The mechanism consisted of two linear actuators, which controlled the pitching and flapping axes independently, attached to moment arms rotating around z and θ axes. In this way, the superposition of pitching and flapping motions could be used to dictate an angle of attack and a gradient in angle of attack independently. The actuator system was designed to accept a timeseries of blade pitch and flap angles, within the maximum actuator velocity and displacement range. As the blade underwent its programmed motion, the flow field around the profile was captured using a 4D-PTV system in order to capture the entire velocity-gradient tensor, and therefore measure vorticity transport [21]. The flow was captured in two adjacent measurement volumes illustrated in Figure 4.

3. Results

The spanwise flow u_r observed in the turbine rotational case increased with convective time for the entire measurement period, as shown in Figure 5. The effective velocity $U_{\text{eff}} = \sqrt{U_{\infty}^2 + \Omega^2 r^2}$ was chosen as the normalization velocity in order to account for the additional flapping velocity. The instantaneous effective velocity was used to normalize the spanwise flow in order to account for the rotational contribution to the effective velocity experienced in the turbine case. The spanwise velocity increased throughout the measurement period as a result of the rotational velocity increasing across the motion. This spanwise flow was on the order of the local rotational velocity Ωr at the measured spanwise position, which is consistent with results found in literature [18, 7]. The direction of spanwise flow is in the direction of decreasing angle of attack for the turbine rotational case, which mirrors that of a wind turbine experiencing a gust event. In comparison, the spanwise flow found in the reference case had a small positive bias indicating nearly two-dimensional flow, with the offset caused by asymmetric boundary conditions.

Similar to the turbine rotational case, the flapping case exhibited increasing spanwise flow u_r within the dynamic stall vortex over the entire measurement period. The spanwise flow was in the same direction as the turbine rotational case, moving from inboard to outboard span locations, due to the pressure gradient induced by rotational accelerations. However, this was in the direction of increasing angle of attack, opposite to that of the turbine rotating case. The spanwise velocity fell within a standard deviation of the turbine case, which indicates that the spanwise flow is not coupled of the angle of attack gradient and is instead a function of the rotational velocity Ω of the blade.

The spanwise vorticity gradient within the dynamic stall vortex is shown in Figure 5. For the turbine case, the gradient decreased towards the tip and becomes increasingly negative as a function of the convective time. This is likely due to the angle of attack gradient along the span of the blade generated during a gust event, which results in an increased circulation generation at inboard spanwise locations. Similar to the spanwise flow, the spanwise vorticity gradient in the two-dimensional case had a small positive bias over the measured period.

Due to the difference in the angle of attack gradient between the turbine and flapping cases, the spanwise vorticity gradient in the flapping case was positive, with vorticity increasing towards the tip. This positive gradient in spanwise vorticity was observed over the entire period of the measurement, and increased as a function of convective time. The magnitude of the spanwise

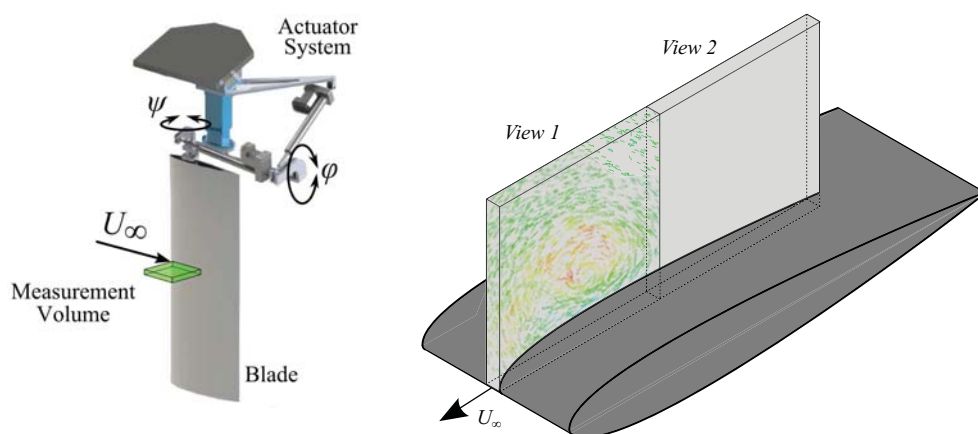


Figure 4. The actuator system is able to actuate the blade in both flapping and pitching (left). The blade motion intersects two adjacent measurement fields of view taken over consecutive runs. An example volumetric vector field is shown, with the profile indicated for scale. (right)

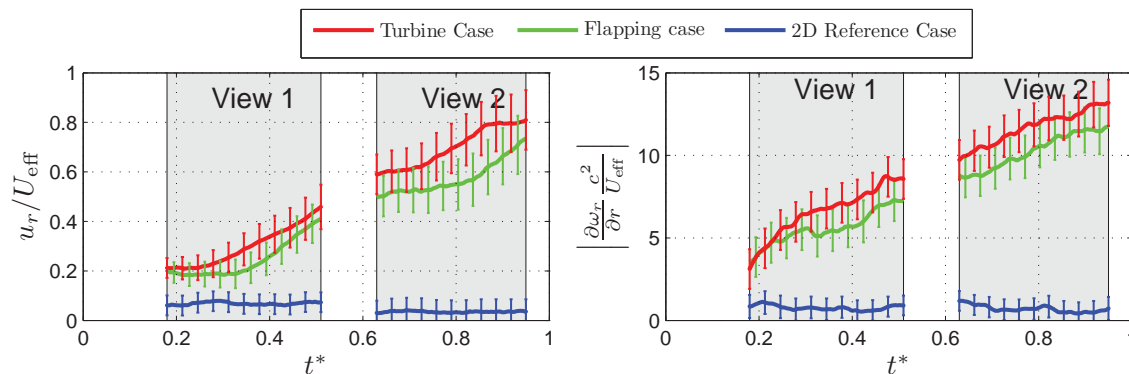


Figure 5. Both the spatially-averaged spanwise flow and vorticity gradient within the dynamic stall vortex was similar between the turbine and flapping cases. In both rotational cases the parameters increase as a function of convective time, for spanwise flow this was on the order of the rotational velocity (Ωr), in close agreement with literature [18]. The reference case exhibited negligible spanwise flow and vorticity gradient. The run-to-run variation was estimated by the standard deviation of the 10 runs, and is plotted every 20 frames.

vorticity gradient fell within one standard deviation between the two rotational cases. For both cases the spanwise gradient in vorticity and angle of attack were the same sign, which agrees with the predicted proportionality between angle of attack and vorticity generation.

Finally, the circulation observed in the turbine case within the measurement volume was greater than that observed for the reference case over the entire measured period, as shown in Figure 6. This indicates that vorticity transport due to the combination of spanwise flow and a spanwise vorticity gradient is acting to redistribute circulation from areas of high circulation generation on the blade to areas of low circulation generation. The relative orientation of the spanwise flow and spanwise vorticity gradient dictates the direction of this transport. The higher levels of circulation growth indicate that locally, the dynamic stall vortex is less stable in the turbine rotational case, and will reach the critical size sooner than the reference case [10].

The observed circulation of the flapping case was lower than the two-dimensional reference case over the entire measurement period. The decrease in circulation is a function of the relative alignment between the spanwise flow and spanwise vorticity gradient generated on the blade. The vorticity gradient in the flapping case was parallel with the spanwise flow, which, based on Equation (8), resulted in circulation being transported from areas of low generation to areas of high generation.

Based on the results from the turbine and flapping cases, it can be observed that in the case of spanwise flow from the root to the tip, a spanwise location with a negative spanwise vorticity gradient, as in the rotational case, experiences increased circulation. This is in contrast to a spanwise location with a positive spanwise vorticity gradient, as in the flapping case, which experiences a decrease in circulation.

4. Conclusion

In this study, the effect of an angle of attack gradient on dynamic stall vortex growth and stability in a rotating system has been investigated. Three cases were considered:

- (i) The turbine case was actuated such that the angle of attack magnitude and spanwise gradient generated on the test model was equivalent to that found at the 30% span of a wind turbine blade experiencing a transient gust event.

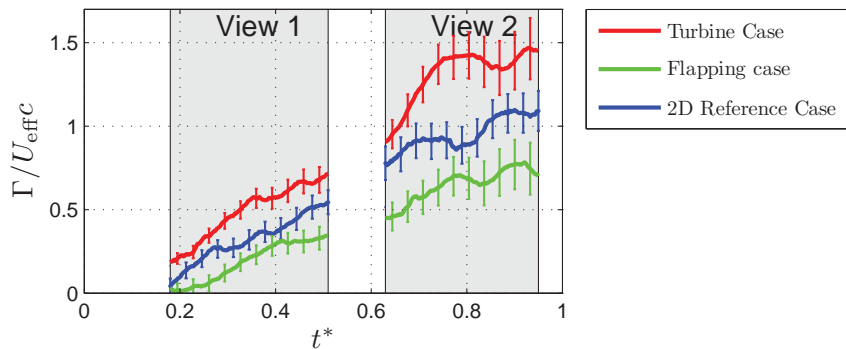


Figure 6. The growth rate of circulation in the turbine case was found to be greater than that of the reference case. In contrast, The growth rate of circulation in flapping case was lower than that of the reference case. The difference in circulation growth is a result of the relative alignment of spanwise flow and the spanwise vorticity gradient between the cases. The error bars denote the standard deviation of the 10 runs plotted every 20 frames.

- (ii) The flapping case was actuated such that the spanwise angle of attack gradient was equal in magnitude, and opposite in direction, relative to the spanwise flow velocity found at the 30% span of a wind turbine blade experiencing a transient gust event.
- (iii) The quasi two-dimensional reference case was actuated in pure pitch such that it had an identical angle of attack history to the rotational cases over the observed convective time.

Two major conclusions have been drawn. First, it has been shown that inducing an angle of attack gradient along the span of the blade results in a corresponding spanwise vorticity gradient. Second, it has been shown that, in combination with a spanwise flow velocity induced from rotational accelerations, the spanwise vorticity gradient results in a redistribution of circulation along the span of the blade, which has an impact on the dynamic loading of turbines in gusty conditions.

4.1. Vorticity Transport and Circulation Redistribution

In the turbine case, the spanwise vorticity gradient was anti-parallel to the spanwise flow, resulting in transport of vorticity from areas of high circulation generation to areas of low circulation generation, increasing the circulation observed. Based on the vortex stability criteria found in literature, the increase in vortex growth rate corresponds to a less stable vortex [10]. Conversely, in the flapping case showed transport of vorticity from areas of low circulation generation to areas of high circulation generation. This effect decreased circulation, indicating increased stability. The decreased vortex stability and increased vortex circulation in the turbine case describes a situation where transient loads increase in frequency and magnitude. Therefore, mitigating the highly transient loads through modifications in either spanwise flow or spanwise vorticity gradient could potentially be an important area of design for increased turbine life.

Under rotation, spanwise flow is induced within the dynamic stall vortex due the spanwise pressure gradient generated from rotational accelerations. The redistribution of circulation through vorticity transport observed was driven by a combination of this spanwise flow and the spanwise vorticity gradient described above. The behaviour of this circulation transport is described by the spanwise convection term $u_r \frac{\partial \omega_r}{\partial r}$ of the vorticity transport equation. The Coriolis term of the vorticity transport equation does not effect the transport of angular

momentum directly. Rather, the Coriolis effect is manifested by inducing a spanwise flow [17]. Therefore, we present an equivalent description of this phenomenon as found in literature, where the circulation-transporting effect of spanwise flow is described through the convection of angular momentum.

References

- [1] Glauert H 1935 *Aerodynamic Theory* vol IV (New York: Springer) 3rd ed
- [2] Burton T, Sharpe D, Jenkins N and Bossanyi E 2001 *Wind Energy Handbook* (Wiley)
- [3] Ronsten G 1992 *J. Wind. Eng. Ind. Aerodyn* **39** 105–118
- [4] Du Z and Selig M 1998 *AIAA* **98**
- [5] Tangler J and Kocurek J D 2005 *43rd AIAA Aerospace Sciences Meeting, Reno, Nevada, USA. AIAA 2005-591*
- [6] Tangler J L 2004 *Wind Energy* **7** 247–260
- [7] Wächter M, Hölling M, Milan P and Joachim P 2011 *AIAA 2011-3299; 6th AIAA Theoretical Fluid Mechanics Conference; Honolulu, Hawaii, USA*
- [8] Hansen K L, Kelso R M and Dally B B 2011 *AIAA journal* **49** 185–194
- [9] Shipley D E, Miller M S and Robinson M 1995 Dynamic stall occurrence on a horizontal axis wind turbine blade Tech. rep. National Renewable Energy Laboratory
- [10] Rival D E, Kriegseis J, Schaub P, Widmann A and Tropea C 2014 *Experiments in Fluids* **55** 1–8
- [11] Ellington C P, van den Berg C, Willmott A P and Thomas A L R 1996 *Nature* **384** 626–630
- [12] Birch J M and Dickinson M H 2001 *Nature* **412** 729–733
- [13] Bomphrey R J, Lawson N J, Harding N J, Taylor G K and L T A 2005 *The Journal of Experimental Biology* **208** 1079–1094
- [14] Lentink D and Dickinson M H 2009 *Journal of Experimental Biology* **212** 2705–2719
- [15] Harbig R R, Sheridan J and Thompson M C 2013 *Journal of Fluid Mechanics* **717** 166–192
- [16] Lentink D and Dickinson M H 2009 *Journal of Experimental Biology* **212** 2691–2704
- [17] Lentink D, Dickson W B, van Leeuwen J L and Dickinson M H 2009 *Science* **324** 1438–1440
- [18] Maxworthy T 2007 *Journal of Fluid Mechanics* **587** 471–475
- [19] Wong J G and Rival D E 2015 *Journal of Fluid Mechanics* **766** 611–625
- [20] Wojcik C J and Buchholz J H J 2014 *Journal of Fluid Mechanics* **743** 249–261
- [21] Schanz D, Gesemann S and Schröder A 2016 *Experiments in Fluids* **57:70**